Available online at www.sciencedirect.com
SCIENCE DIRECT®
Vibrational Spectroscopy 35 (2004) 67–76
VIBRATIONAL SPECTROSCOPY
www.elsevier.com/locate/vibspec

Modelling IR-spectra of single-phase polycrystalline materials with random orientation—a unified approach

Thomas G. Mayerhöfer*

Institut für Physikalische Chemie, Friedrich-Schiller-Universität Jena, Lessingstraße 10, D-07743 Jena, Germany

Received 10 October 2003; received in revised form 17 November 2003; accepted 18 November 2003

Available online 17 January 2004

Abstract

Two recently developed formalism, one for the modelling of spectra of randomly oriented polycrystalline bulk materials consisting exclusively of crystallites being small compared to the resolution limit [Appl. Spectrosc. 56 (2002) 1194] and one for polycrystalline bulk materials in the large crystalline limit [J. Opt. A: Pure Appl. Opt. 4 (2002) 540] are combined in a unified approach in order to enable the modelling of spectra of materials consisting of both optically small and large regions of order. Based on this generalized formalism, several model calculations are carried out to demonstrate the influence of different crystallite size distribution on IR-reflectance spectra. The model calculations for a sample consisting of a 3:1 mass mixture of small and large crystallites are compared with the experimental results; the good correspondence between measured and modeled spectra confirms the value of the unified approach.

Keywords: Infrared; Optical properties; Birefringence; Random orientation; Polycrystalline bulk materials; Size effect

1. Introduction

Before a meaningful quantitative interpretation of the spectra of bulk polycrystalline materials is possible, the inverse problem must be solved, which consists of modelling these spectra from single crystal data. It is well known that the spectra of powdered materials are strongly influenced by a broad variety of parameters like, e.g. particle size, particle shape and the kind of the embedding medium [1–4]. Less well effort has been spent on the understanding of the (infrared) optical properties of polycrystalline randomly oriented bulk materials consisting of anisotropic crystallites. They were routinely interpreted based on the apparent equivalence of the terms ''optical isotropy'' and ''cubic symmetry'' [5]. Therefore, it is assumed that the spectra of randomly oriented polycrystalline materials can be interpreted by performing a dispersion analysis, which seems to allow obtaining the oscillator parameters. These parameters are connected directly with the structure of the material on an atomic level if they stem from oriented single crystal spectra. Unfortunately, dispersion analysis of the spectra of polycrystalline materials is not capable of providing meaningful oscillator parameters in general, since conventional dispersion analysis assumes an arithmetic average of the principle dielectric functions of the ordered regions and this kind of average has been shown to be inadequate [6]. Besides, the shape of bands in the infrared is considerably altered for polycrystalline materials with crystallite diameter $d < \lambda/10$ compared to the typical Lorentzian shape. It generally consists of a sharp maximum at the TO-wavenumber of the corresponding oscillator with a broadening at the high wavenumber side due to the excitation of mixed TO–LO modes [6]. For $d > \lambda/10$ the concept of an averaged dielectric function or an averaged index of refraction completely fails, since the spectra of such materials exhibit, e.g. non-zero cross-polarization terms despite of being optically isotropic. Instead of, it is necessary to average the reflectance or transmittance of a single crystallite over all possible orientations in order to model the reflectance or transmittance spectra of the polycrystalline sample [7,8]. An analogous non-coherent averaging can be carried out with similar success to explain, e.g. the VIS optical properties of polymer-dispersed multi domain structured cholesteric liquid crystals [9,10].

In general, it is unlikely that samples consist of optically small or large crystallites exclusively. It is therefore desirable to have an approach which is able to predict the spectra of single-phase bulk polycrystalline materials consisting of both small and large crystallites. This approach, which is not

* Tel.: +49-3641-948-314; fax: +49-3641-948-302.
E-mail address: thomas.mayerhoefer@uni-jena.de (T.G. Mayerhöfer).

0924-2031/$ – see front matter © 2003 Elsevier B.V. All rights reserved.
doi:10.1016/j.vibspec.2003.11.011

limited to the IR-spectral region on principle, consists of a combination of two recently published theories [6,7] with similar underlying concepts and is introduced in Section 2. Modeled spectra for several different crystallite size distributions and comparisons between experiment and theory are given in Section 3. The paper concludes with a summary and a short discussion of the results with regard to the interpretation of the infrared spectra of polycrystalline single-phase materials.

2. Theory

In the following a bulk polycrystalline material will be considered as an ensemble of independent microscopic single crystals with arbitrary orientations Ω. Each of the microscopic single crystals shall be non-magnetic ($\mu = 1$) and shall possess the same in general complex dielectric tensor ε as its macroscopic counterpart.

Assuming that a two-dimensional square grid (grid constant g_c equals the theoretical resolution power of light, $g_c = \lambda/10$) is placed on the surface of a bulk polycrystalline material (compare Fig. 1), four different principal situations, presented in Fig. 2, can be discussed.

(a) The dimensions of the crystallites (or ordered regions) are much smaller than the resolution limit. Since the crystals are randomly oriented, the possible orientations form a continuous distribution within every single grid-square.
(b) The dimensions of the crystallites are smaller than $\lambda/10$. In a single grid-square the orientations form a discrete distribution.
(c) The dimensions of the crystallites are larger than $\lambda/10$. The orientations of the crystals are continuously distributed referring to the area under inspection.
(d) All crystals possess the same orientation or the material is single-crystalline.

The last mentioned case has been treated by several authors before [11–15]. The reader is therefore referred to the literature for details.

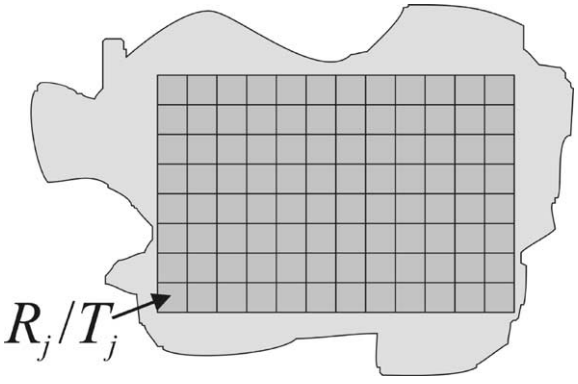

Fig. 1. Illustration of the model concept which underlies Eq. (1).

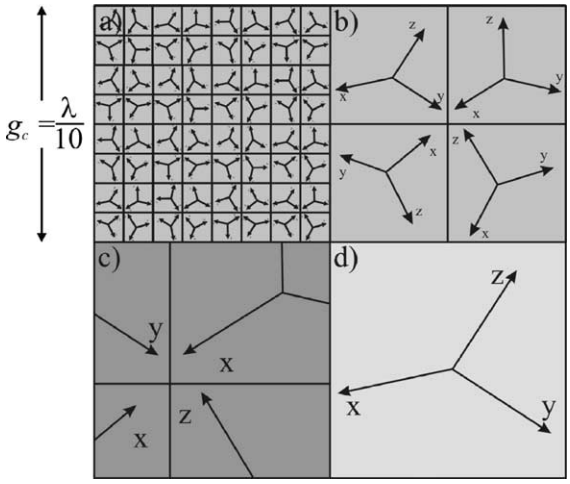

Fig. 2. Principal limiting cases in the IR-spectroscopy of polycrystalline materials: (a) all crystallites/regions of order much smaller than the grid constant g_c (the resolution limit), continuous distribution of orientations within one grid-square, (b) crystallite diameter smaller than g_c, (c) crystallites larger than g_c (continuous distribution of orientations within the area under inspection) and (d) all crystallites have the same orientation.

The following derivations will be carried out under the constraint of negligible scattering effects (smooth surfaces). Therefore, any attenuation of the incident light is based only on specular reflection and absorption.

In the most general case reflectance or transmittance is given as the average of reflectance/transmittance contributed from every single grid-square assuming a non-coherent light source:

$$\langle R\rangle = N\sum_{j=1}^{K} R_j, \qquad \langle T\rangle = N\sum_{j=1}^{K} T_j \tag{1}$$

K denotes the total number of grid-squares in Eq. (1) and N a normalization factor ($N = K^{-1}$). This summation can be split up in principle in parts belonging to the limiting cases (a)–(c), which must be weighed according to their fractional part of the surface area under inspection (the limiting cases will be discussed separately below). This is reflected in the following equivalent representation of Eq. (1):

$$\langle R\rangle = \frac{\int_{d_{\min}}^{d_{\max}} a_r(d)R(d)\,\mathrm{d}d}{A}, \qquad \langle T\rangle = \frac{\int_{d_{\min}}^{d_{\max}} a_r(d)T(d)\,\mathrm{d}d}{A} \tag{2}$$

Here, $a_r(d)$ denotes the fractional part of the surface area occupied by crystallites with crystallite diameter d and A is the total area under inspection.

The optical properties of a crystal can be specified by its complex dielectric tensor ε. In the intrinsic coordinate system x, y, z of the crystal ($x\|a$, $y\|b$, $z\|c$; a, b, c are the crystallographic axes) the dielectric tensor is given by

$$\varepsilon = \begin{pmatrix} \varepsilon_a & 0 & 0 \\ 0 & \varepsilon_b & 0 \\ 0 & 0 & \varepsilon_c \end{pmatrix}, \tag{3}$$

where ε_a, ε_b and ε_c are the principal dielectric constants. Relative to a reference frame (e.g. the laboratory coordinates X, Y, Z) the dielectric tensor is given in general by

$$\varepsilon(X,Y,Z) = \boldsymbol{A}(\Omega)\begin{pmatrix}\varepsilon_a & 0 & 0\\ 0 & \varepsilon_b & 0\\ 0 & 0 & \varepsilon_c\end{pmatrix}\boldsymbol{A}(\Omega)^{-1}. \quad (4)$$

Here, $\boldsymbol{A}$ is a rotation matrix depending on the orientation Ω, which may be specified, e.g. by one of the 24 Euler orientation representations.

The material property $\varepsilon(X, Y, Z)$ is closely related to the wavevector $\vec{k}$ inside the medium under inspection. This linkage can be described by several equivalent formalisms. One of these is the well-known Fresnel's formula [5]; another one has been utilized by Yeh [12], which is adopted in the following.

Say, the X–Z-plane of laboratory coordinate system is chosen as the plane of incidence. Consequently, the angle between the ray direction and the Z-axis is the angle of incidence α. Then, the Z-component of $\vec{k}$ inside the medium, γ, can be calculated solving Eq. (5) [12],

$$\det\left|\begin{pmatrix}\varepsilon_{XX}-\sin^2\alpha-\gamma^2 & \varepsilon_{XY} & \varepsilon_{XZ}\\ \varepsilon_{YX} & \varepsilon_{YY}-\gamma^2 & \varepsilon_{YZ}+\gamma\sin\alpha\\ \varepsilon_{ZX} & \varepsilon_{ZY}+\gamma\sin\alpha & \varepsilon_{ZZ}-\sin^2\alpha\end{pmatrix}\right| = 0 \quad (5)$$

resulting in a quadratic equation in γ with four solutions $\gamma_{\pm1}$ and $\gamma_{\pm2}$:[1]

$$\begin{aligned}
\gamma_{\pm1} &= -\tfrac{1}{2}K_8 \pm \tfrac{1}{2}\left(\sqrt{K_9} \pm \sqrt{2K_9 - K_7 \pm K_{10}}\right)\\
\gamma_{\pm2} &= -\tfrac{1}{2}K_8 \pm \tfrac{1}{2}\left(\sqrt{K_9} \mp \sqrt{2K_9 - K_7 \pm K_{10}}\right)\\
K_1 &= \sin\alpha\left(\varepsilon_{XY}\varepsilon_{XZ} + \sin^2\alpha\,\varepsilon_{YZ} - \varepsilon_{XX}\varepsilon_{YZ}\right)\\
K_2 &= \sin^2\alpha\left(\varepsilon_{YY}+\varepsilon_{ZZ}\right) + \varepsilon_{XZ}^2 + \varepsilon_{YZ}^2 - \varepsilon_{XX}\varepsilon_{ZZ} - \varepsilon_{YY}\varepsilon_{ZZ}\\
K_3 &= \sin^2\alpha\left(\varepsilon_{XY}^2 + \sin^2\alpha\,\varepsilon_{YY} - \varepsilon_{XX}\varepsilon_{YY} + \varepsilon_{YZ}^2 - \varepsilon_{YY}\varepsilon_{ZZ}\right)\\
&\quad - \varepsilon_{XZ}^2\varepsilon_{YY} + 2\varepsilon_{XY}\varepsilon_{XZ}\varepsilon_{YZ} - \varepsilon_{XX}\varepsilon_{YZ}^2 - \varepsilon_{XY}^2\varepsilon_{ZZ} + \varepsilon_{XX}\varepsilon_{YY}\varepsilon_{ZZ}\\
K_4 &= K_2^2 + 12\left(\varepsilon_{ZZ}K_3 - \sin\alpha\varepsilon_{YZ}K_1\right)\\
K_5 &= \varepsilon_{ZZ}\left(108K_1^2 - 72K_2K_3\right)\\
&\quad - \sin\alpha\,\varepsilon_{YZ}\left(36K_1K_2 - 108\sin\alpha\,\varepsilon_{YZ}K_3\right) + 2K_2^3\\
K_6 &= \left(K_5 + \sqrt{{K_5}^2 - 4K_4^3}\right)^{1/3}\\
K_7 &= \frac{\sqrt[3]{2\varepsilon_{ZZ}^3}K_4}{\varepsilon_{ZZ}^2K_6} + \frac{K_6}{\sqrt[3]{2\varepsilon_{ZZ}^3}}\\
K_8 &= \frac{\sin\alpha\,\varepsilon_{YZ}}{\varepsilon_{ZZ}}\\
K_9 &= K_8^2 - \frac{1}{3}\left(\frac{2K_2}{\varepsilon_{ZZ}} - K_7\right)\\
K_{10} &= \frac{8\left(K_8K_2 - \varepsilon_{ZZ}K_8^3\right) - 16K_1}{4\varepsilon_{ZZ}\sqrt{K_9}}
\end{aligned} \quad (6)$$

[1] Here, we abstain from presenting analytic expressions containing angular orientations due to the multitude of different orientation representations (Euler angle orientation representations, symmetric Euler orientation representations, reparameterized quaternions, etc.) not all of which are equally appropriate for orientational averaging. For optically uniaxial materials expressions containing angular orientations can be found in [6].

Explicit analytic expressions for γ have been given previously in references [13,16] (Additionally, Abdulhalim [16] presents a more general form of Eq. (6) for arbitrary incidence and also explicit solutions for certain special cases). The form given here is optimized for fast computer calculations.

The eigenvectors belonging to $\gamma_{\pm1}$ and $\gamma_{\pm2}$ are the polarization directions inside the crystal. From these eigenvectors a transfer matrix $\boldsymbol{M}$ can be computed, which links the amplitudes of the incident, reflected and transmitted waves:

$$\begin{pmatrix}A_s\\ B_s\\ A_p\\ B_p\end{pmatrix} = \begin{pmatrix}M_{11} & M_{12} & M_{13} & M_{14}\\ M_{21} & M_{22} & M_{23} & M_{24}\\ M_{31} & M_{32} & M_{33} & M_{34}\\ M_{41} & M_{42} & M_{43} & M_{44}\end{pmatrix}\begin{pmatrix}C_s\\ 0\\ C_p\\ 0\end{pmatrix} \quad (7)$$

Here A_s and A_p are the field amplitudes of the incident beam with perpendicularly (s-) and parallelly (p-)polarized radiation, respectively. Analogously, B and C denote the amplitudes of the reflected and transmitted waves. The reflection and transmission coefficients r_{ss} and t_{ps} are calculated, e.g. as follows:

$$\begin{aligned}
r_{ss} &= \left(\frac{B_s}{A_s}\right)_{A_p=0} = \frac{M_{21}M_{33} - M_{23}M_{31}}{M_{11}M_{33} - M_{13}M_{31}},\\
t_{ps} &= \left(\frac{C_s}{A_p}\right)_{A_s=0} = \frac{-M_{13}}{M_{11}M_{33} - M_{13}M_{31}}
\end{aligned} \quad (8)$$

and three additional equations for each [12]. If, for example, only the incident wave is s-polarized, the corresponding reflectance R_s can be calculated according to Eq. (10):

$$R_s = R_{ss} + R_{sp} = |r_{ss}|^2 + |r_{sp}|^2 \quad (9)$$

2.1. Large crystallite limit—average reflectance and transmittance theory (ARTT)

This case has been treated in detail in references [7,8]. Eq. (1) takes on the following form,

$$\begin{aligned}
\langle R\rangle &= N^{(3)}\int_{\Omega^{(3)}} R(\Omega)\,\mathrm{d}\Omega = N^{(3)}\int_{\Omega^{(3)}}\left(\tfrac{1}{2}R_s(\Omega) + \tfrac{1}{2}R_p(\Omega)\right)\mathrm{d}\Omega\\
\langle T\rangle &= N^{(3)}\int_{\Omega^{(3)}} T(\Omega)\,\mathrm{d}\Omega = N^{(3)}\int_{\Omega^{(3)}}\left(\tfrac{1}{2}T_s(\Omega) + \tfrac{1}{2}T_p(\Omega)\right)\mathrm{d}\Omega
\end{aligned}, \quad (10)$$

where $R(\Omega)$ and $T(\Omega)$ are calculated according to the preceding section and $N^{(3)}$ is a normalization factor given by

$$N^{(3)} = \left(\int_{\Omega^{(3)}}\mathrm{d}\Omega\right)^{-1}.$$

2.2. Discrete distribution of orientation within the grid-squares

If the crystallites are strongly absorbing as in the Reststrahlen region the penetration depth may be of order of the

dimensions of a crystallite or even smaller. Therefore, only the first layer of crystallites contributes to the reflectance of the sample. Then, in certain wavenumber ranges, the number of crystallites inside a square according to Fig. 1 may be too small as to consider the distribution of orientations within every single grid-square to be continuous. According to the average refractive index theory (ARIT) [6], this situation can be simulated by averaging the indices of refraction for a discrete number of random orientations. The indices of refraction are obtained by solving Eq. (5) while setting $\alpha = 0$:

$$\det\left|\begin{pmatrix} \varepsilon_{XX}-\gamma^2 & \varepsilon_{XY} & \varepsilon_{XZ} \\ \varepsilon_{YX} & \varepsilon_{YY}-\gamma^2 & \varepsilon_{YZ} \\ \varepsilon_{ZX} & \varepsilon_{ZY} & \varepsilon_{ZZ} \end{pmatrix}\right| = 0 \tag{11}$$

From Eq. (11) four solutions for γ result, two of which belong to forward travelling waves (γ_{+1}, γ_{+2}) and the other two to backward travelling waves (γ_{-1}, γ_{-2}) [6]:

$$\begin{aligned} \gamma_{\pm1} &= \pm\sqrt{K_1 - \frac{1}{2\varepsilon_{ZZ}}\sqrt{K_2 - 4K_3}} \\ \gamma_{\pm2} &= \pm\sqrt{K_1 + \frac{1}{2\varepsilon_{ZZ}}\sqrt{K_2 - 4K_3}} \\ K_1 &= \frac{1}{2}\left(\varepsilon_{XX} + \varepsilon_{YY} - \frac{\varepsilon_{XZ}\varepsilon_{ZX} + \varepsilon_{YZ}\varepsilon_{ZY}}{\varepsilon_{ZZ}}\right) \\ K_2 &= (\varepsilon_{XZ}\varepsilon_{ZX} + \varepsilon_{YZ}\varepsilon_{ZY} - \varepsilon_{XX}\varepsilon_{ZZ} - \varepsilon_{YY}\varepsilon_{ZZ})^2 \\ K_3 &= \varepsilon_{ZZ}(\varepsilon_{XX}\varepsilon_{YY}\varepsilon_{ZZ} + \varepsilon_{XY}\varepsilon_{YZ}\varepsilon_{ZX} + \varepsilon_{XZ}\varepsilon_{YX}\varepsilon_{ZY} \\ &\quad -\varepsilon_{XX}\varepsilon_{YZ}\varepsilon_{ZY} - \varepsilon_{XY}\varepsilon_{YX}\varepsilon_{ZZ} - \varepsilon_{XZ}\varepsilon_{YY}\varepsilon_{ZX}) \end{aligned} \tag{12}$$

The solutions γ_{+1} and γ_{+2}, which have a positive sign if they are real (otherwise their imaginary parts are positive), equal the two indices of refraction n_1 and n_2.

The averaged index of refraction is then given by

$$\langle n\rangle_j = N\sum_{i=1}^{k}\left(\tfrac{1}{2}n_1(\Omega_i) + \tfrac{1}{2}n_2(\Omega_i)\right) \tag{13}$$

where k is the number of crystallites inside a grid-square. Since $k\epsilon\mathbb{N}$ and simultaneously $k = k(\tilde{\nu})$, the value of k must hold for a range of wavenumbers in computations. The reflectance R_j of every grid-square is then calculated by Fresnel's formula [5]. Subsequently, all R_j are averaged according to Eq. (3). The aforementioned case is, as will be shown later, of lower practical importance since $\langle R\rangle$ and $\langle T\rangle$ are very similar to the values calculated with ARIT for values of $k > 10$ if a sufficiently large value of K (the number of grid-squares) is chosen.

2.3. Small crystallite limit (ARIT)

In case of a continuous distribution of orientations the average index of refraction is given by [6]

$$\langle n\rangle_j = N^{(3)}\int_{\Omega^{(3)}}\left(\frac{n_1(\Omega)}{2} + \frac{n_2(\Omega)}{2}\right)\mathrm{d}\Omega. \tag{14}$$

Again, as in the preceding case, the reflectance R_j and the transmittance T_j are calculated according to Fresnel's formula [5] and the averages $\langle R\rangle$ and $\langle T\rangle$ are obtained following Eq. (3). In practice, the integral cannot be solved analytically. Therefore, a numerical evaluation of the Integral is required and Eq. (14) is replaced by Eq. (13). Due to a relatively strong convergence even in case of great differences of the principal dielectric functions [6], it will be sufficient to choose the number of crystallites within one grid-square k or the number of different orientations Ω chosen randomly equal to about 144 if $K = 1$ (compare reference [6]). The same applies to the integral which has to be evaluated in the large crystallite limit (Eq. (10)) [7]. In principle, it would be feasible to replace ARIT by another applicable theory like, e.g. the effective medium approximation (EMA). This substitution would be, however, on expense of the loss of the similar structure as exposed by ARIT and ARRT.

3. Results and discussion

3.1. The limiting cases

We will first shortly discuss the results if the approach given in Section 2 is applied to the limiting cases (a)–(c) which were introduced in the preceding section. The cases (a) ($d \ll \lambda/10$) and (c) ($d > \lambda/10$) were already treated in a detailed way in [6–8], respectively. As in these references, we decided to show the results for polycrystalline fresnoite ($Ba_2TiSi_2O_8$). Fresnoite is optically uniaxial with in general relatively large differences between its principal dielectric functions in the Reststrahlen range and is therefore well-suited for this purpose [17]. Apart from the single crystal and randomly oriented polycrystalline samples it was also investigated in form of oriented glass ceramics by means of IR-reflectance spectroscopy [18] and is therefore a well-characterized material in the infrared spectral range.

The principal dielectric functions employed for the modelling were derived from single crystal spectra with help of the classical three parameter dielectric function model [17],

$$\varepsilon_j(\tilde{\nu}) = \varepsilon_{\infty j} + \sum_{i=1}^{N}\frac{S_{ij}^2}{(\tilde{\nu}_{ij}{}^2 - \tilde{\nu}^2) - i\tilde{\nu}\gamma_{ij}} \quad j = a, c \tag{15}$$

where S_{ij} is the oscillator strength of the ith oscillator, $\tilde{\nu}_{ij}$ and γ_{ij} its position and its damping constant, respectively, and $\varepsilon_{\infty j}$ the dielectric background. Details of the fitting procedure and a comparison between calculated and measured spectra of the single crystal exhibiting excellent agreement between both can be found in [17]. Since the parameter obtained by the fitting procedure and used to generate the principal dielectric functions have not been reported so far, they are given in Table 1.

Being optical uniaxial, the orientation of a fresnoite crystallite can be specified unambiguously by two Euler

Table 1
Oscillator parameter used to generate the principal dielectric functions ε_a and ε_c of fresnoite according to Eq. (15) in the infrared spectral range (in cm^{-1})

i	ε_a			ε_c		
	$\tilde{\nu}_{ia}$	S_{ia}	γ_{ia}	$\tilde{\nu}_{ic}$	S_{ic}	γ_{ic}
1	121.5	113.3	5.7	141.3	195.3	11.7
2	165.7	105.4	11.5	150.9	127.1	9.2
3	184.3	46.0	9.9	222.6	101.7	24.8
4	274.2	144.3	12.5	231.2	86.1	8.6
5	376.9	511.5	8.9	262.7	40.7	11.4
6	394.5	222.7	29.4	282.9	80.5	11.5
7	478.5	215.4	7.2	475.3	84.3	13.7
8	498.3	29.7	8.3	583.2	292.5	8.1
9	538.7	43.8	19.0	662.6	130.6	8.6
10	580.4	98.6	12.6	857.9	323.8	11.5
11	748.8	69.2	12.4	952.8	297.6	12.0
12	860.4	378.4	11.4	1024.6	503.9	9.5
13	902.1	554.3	10.4			
14	965.3	201.2	11.4			
15	1006.1	66.2	39.1			
$\varepsilon_{\infty j}$	3.006			3.032		

angles φ, θ and $d\Omega$ can therefore be given by $d\varphi\, d\theta$ in this case (often the relation $d\Omega = \sin\theta\, d\varphi\, d\theta$ can be found in literature; for a discussion of this problem see [6,8]). The values of these angles take on all values from 0 to $\pi/2$ assuming a continuous distribution of orientations (in the large crystallite limit, it is necessary that θ ranges from 0 to π if $\alpha \neq 0^\circ$ [8]). In general, the integrals in Eqs. (10) and (14) have no analytical solution and must consequently be replaced by summations. The simulated spectra in Fig. 3(a) and (c) had been computed assuming an evenly spaced distribution of the angles φ and θ, while for the calculation of the spectra shown in Fig. 3b), the orientations were chosen in a random manner. The same Monte Carlo related method was adopted for the calculation of all following simulated spectra. In Fig. 3b) the spectra for four virtual samples of fresnoite were simulated assuming the same constant number k of regions of order within every grid-square independent of wavelength. While this assumption is of course not valid or not applicable in practice (only in limited wavenumber ranges), it is necessary to compare the results with the spectrum computed for the small crystallite limit. Obviously, the spectra are all similar with minor (except for $k = 1$) differences at the high wavenumber side, especially in case of the bands above 900 cm^{-1}, which disappear with increasing number of crystallites per grid-square: If $k = 10$, there is virtually no difference to case (a) (small crystallite limit). Taking into account the relatively strong optical anisotropy of fresnoite, which emphasizes the size effects, case (b) seems to be of less importance especially for weakly absorbing materials due to non-negligible contributions from deeper layers of crystallites.

The agreement between simulated and measured spectrum is quite satisfactorily in the small crystallite limit ($d < 800$ μm) as is illustrated in Fig. 3a) and even gets better, if the damping constants of the single crystal are slightly varied with a *common* factor of about 1.3 [6] (this factor was evaluated by the comparison of the simulated and the ''measured'' complex part of the dielectric function. The simulation was based on the (varied) single crystal data, and was compared to data evaluated from the measured spectrum of the polycrystalline material by dispersion analysis. A direct comparison of the reflectance spectra favors a factor of about 1.25 [19]). Such a common factor could not be utilized if effective medium approximation (EMA) was

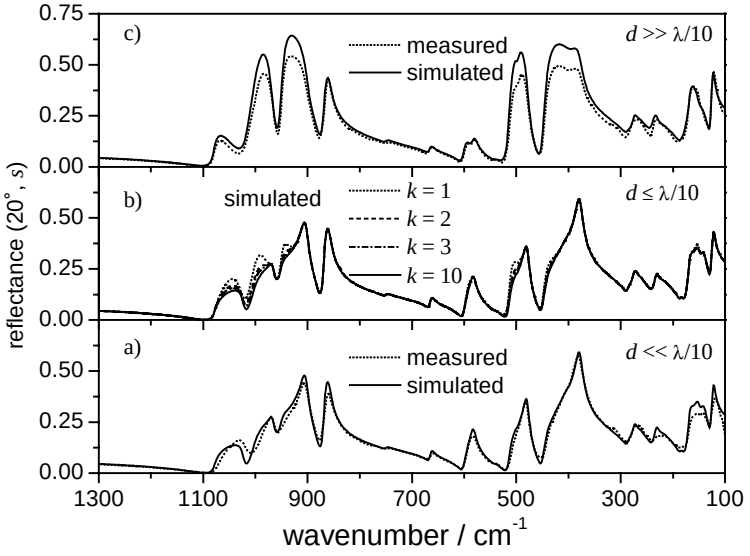

Fig. 3. Measured and simulated reflectance spectra of randomly oriented polycrystalline fresnoite consisting exclusively of optically small (a) or large crystallites (c) ($\Delta\varphi = \Delta\theta = 1^\circ$, homogenous distribution of orientations) and simulated spectra of virtual samples with 1, 2, 3 and 10 crystallites inside every grid-square (b), computed assuming 10^4 different grid-squares with randomly oriented crystallites).

used. The coincidence between measured and simulated spectrum of a polycrystalline fresnoite sample in the large crystallite limit (average crystallite diameter ≈ 10 μm) is not as good as in the preceding example due to scattering losses from the comparably rough surface of this sample include a hint of Fig. 3C). However, the most important features like band shapes and the situations of the peak maxima are satisfactorily well reproduced (the resemblance between measured and modeled spectra referring to band shapes is improved, if all damping constants of the single crystal are multiplied by 1.1 [8]). As was already stated (compare Section 2), the utilization of a non-coherent averaging scheme is justified by the employment of non-coherent light sources [9,10]. Calculations with a coherent averaging scheme (averaging over the reflection coefficients, compare Eq. (8)) show that it is not necessary to consider coherent averaging in the particular case of interest in agreement with the results given in references [7–10] since band profiles and relative and absolute reflectance values are changed considerably by the coherent averaging scheme towards lower resemblance between modeled and measured spectra (results are not shown).

The strong differences between the spectra of the samples with small and large crystallites, respectively, clearly demonstrate the importance of taking into account this anisotropy-based size effect for the interpretation of the spectra. Additionally, the use of an exact 4×4-matrix algorithm for the calculation of spectra of samples in the large crystallite limit revealed an unknown optical property of these samples, which was confirmed experimentally [7,8], namely the ability to depolarize light. In general, the following relations hold [7]:

$$R_{\mathrm{ps}}(\Omega) \geq 0, \quad R_{\mathrm{sp}}(\Omega) \geq 0; \qquad T_{\mathrm{ps}}(\Omega) \geq 0, \quad T_{\mathrm{sp}}(\Omega) \geq 0; \tag{16}$$

Assumed that $\varepsilon_{\mathrm{a}} \neq \varepsilon_{\mathrm{b}} \neq \varepsilon_{\mathrm{c}}$, the cross-polarization terms R_{ps}. R_{sp}, T_{ps}, T_{sp} are zero only for high symmetry orientations of the crystallites (the principal axes of the tensor ellipsoid of a crystallite are oriented parallel and perpendicular, respectively, to the polarization direction of the incident radiation).

Therefore, the non-zero cross-polarization of randomly oriented materials with $d > \lambda/10$ follows readily from the applied averaging scheme (Eq. (10) in combination with Eq. (9)):

$$\begin{aligned}
\langle R_{\mathrm{ps}} \rangle &= N^{(3)} \textstyle\int_{\Omega^{(3)}} R_{\mathrm{ps}}(\Omega)\, \mathrm{d}\Omega > 0 \\
\langle R_{\mathrm{sp}} \rangle &= N^{(3)} \textstyle\int_{\Omega^{(3)}} R_{\mathrm{sp}}(\Omega)\, \mathrm{d}\Omega > 0 \\
\langle T_{\mathrm{ps}} \rangle &= N^{(3)} \textstyle\int_{\Omega^{(3)}} T_{\mathrm{ps}}(\Omega)\, \mathrm{d}\Omega > 0 \\
\langle T_{\mathrm{sp}} \rangle &= N^{(3)} \textstyle\int_{\Omega^{(3)}} T_{\mathrm{sp}}(\Omega)\, \mathrm{d}\Omega > 0
\end{aligned} \tag{17}$$

It must be stated that the existence of non-zero cross-polarization terms is not necessarily connected with linear dichroism. Also in regions were the principal indices of refraction are real numbers, a distinction between large and small crystallites is possible in principal, provided that they differ. Unfortunately, these differences have to be relatively large to cause, e.g. a cross-polarization above the detection limit if conventional instrumentation is utilized. For fresnoite, the difference amounts to $\Delta n \approx 0.14$ at 1500 cm^{-1} leading to a calculated cross-polarization $R_{\mathrm{sp}} = R_{\mathrm{ps}} = 4 \times 10^{-5}$ (assuming that $k_{\mathrm{a}} = k_{\mathrm{c}} = 0$, where k_i is the imaginary part of the principal refractive index belonging to axis i), while measurements of the cross-polarization of a polycrystalline fresnoite sample with small crystallites ($d < 400$ nm) show an average value of about 6×10^{-4} in the spectral range from 1450 to 1550 cm^{-1} indicating an error of the same order (Bruker IFS 66, wire grid polarizers on KRS-5), since the cross-polarization of such a sample should equal zero.

The existence of non-zero cross-polarization terms clearly demonstrates the impossibility to describe the optical properties of randomly oriented polycrystalline materials with large crystallites with a scalar dielectric function.

3.2. Simulated spectra of three different crystallite size distributions

In the following, simulated spectra for three different kinds of crystallite size distributions will be discussed. First, we will assume that the samples consist of a constant ratio of large and small crystallites in the wavenumber range of interest. The corresponding representation is shown in Fig. 4. For fresnoite this will limit our discussion in the main to crystallites smaller than about 300 nm and larger than 10 μm with the underlying assumption that the resolution limit equals $\lambda/10$. For small crystallites the upper limit is then based on the high wavenumber limit of the Reststrahlen bands (about 1100 cm^{-1}) and the condition that the number of crystallites inside one grid-square $k = 10$.

From Eqs. (1) and (2) it follows that the simulated spectra depicted in Fig. 4 can be calculated by

$$R = a_{\mathrm{r}}(\mathrm{large})R(\mathrm{large}) + [1 - a_{\mathrm{r}}(\mathrm{large})]R(\mathrm{small}), \tag{18}$$

where a_{r}(large) does not depend on wavelengths and is denoted simply a_{r} in Fig. 4. As a consequence of Eq. (18), the cross-polarized reflectance at a fixed wavenumber increases linearly with a_{r}, during R_{s} transforms from R_{s}(small) to R_{s}(large). The transformation is most distinct in the ranges between 350 and 450 cm^{-1} and 900 and 1100 cm^{-1}, while between 680 and 880 cm^{-1} fresnoite is nearly optically isotropic and, as a consequence, only small changes are detectable in this range. Overall, a determination of the fractional part a_{r} should be possible in general.

The basic assumptions that underlie the second distribution are that $\mathrm{d}a_r(d)/\mathrm{d}d = 0$ (each fraction occupies the same volume) and that the growth of the crystallites stopped at $d_{\max}$. The accordingly simulated spectra are shown in Fig. 5. For the simulations a program was utilized, which is based on a numerical approximation of the integral in Eq. (2). It first calculates for a fixed d the number of crystallites k within a grid-square for a given wavenumber. If $k < 1$ the

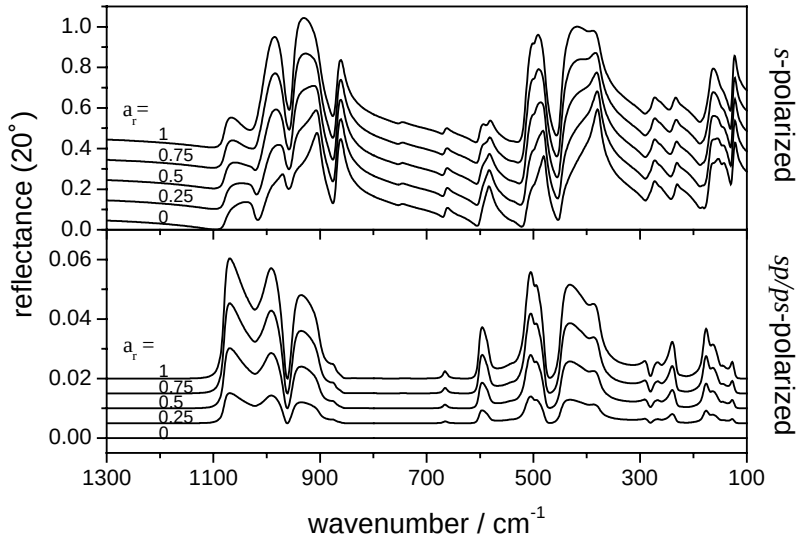

Fig. 4. Simulated reflectance spectra of randomly oriented polycrystalline fresnoite consisting of both optically small ($d \ll \lambda/10$) and large crystallites ($d > \lambda/10$) in different proportions, which are independent of wavenumber by assumption (incidence angle 20°, the spectra are shifted for clarity). a_r is the fractional part of the surface area occupied by large crystallites. Upper part: perpendicularly polarized incident radiation (shift: 0.1); lower part: cross-polarization (shift: 0.005).

crystallite is considered as large and the reflectance is calculated according to Eq. (10), otherwise an averaged index of refraction is computed according to Eq. (13) and the reflectance is calculated from the Fresnel equation. This is done for the whole range of wavenumbers of interest. The calculation is then repeated for different diameters according to a specified range and step size of d. In the last step the results are averaged using an appropriate weighing factor $a_r(d)$.

It is obvious from Fig. 5 that the R_s-spectrum belonging to $d_{max} = 5$ μm is above 600 cm^{-1} relatively similar to the spectrum of the sample consisting completely of large crystallites. However, as could be expected, the bands located around 163 and 385 cm^{-1} show noticeable differences referring to the band shapes. Additionally, there exist small differences of the band intensities, which increase with decreasing wavenumber, especially in the cross-polarized reflectance spectra. From these spectra d_{max} can be evaluated simply, since the intensity of the cross-polarized reflectance drops abruptly to zero, if the resolution limit becomes larger than d_{max} according to the theory given in Section 2. Concerning this, however, it must be emphasized that it

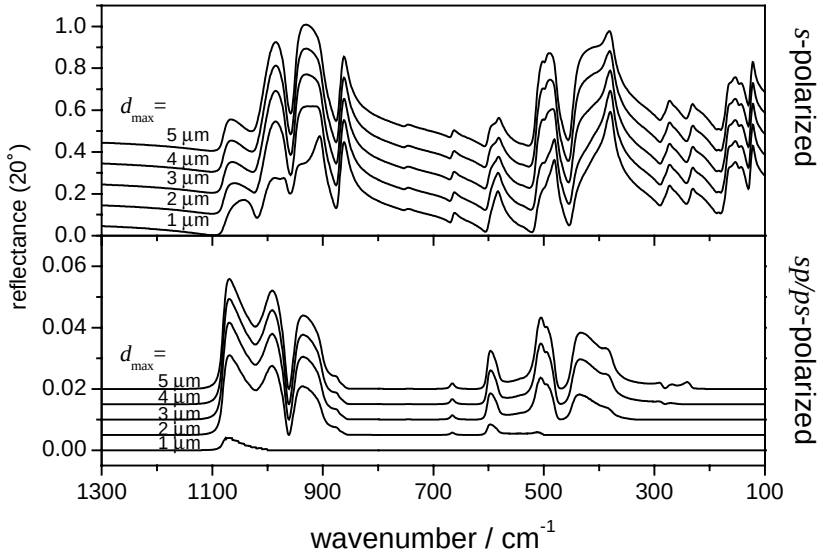

Fig. 5. Simulated reflectance spectra of randomly oriented polycrystalline fresnoite assuming that each size-fraction occupies the same volume and that the growth of the crystallites stopped at d_{max} (incidence angle 20°, the spectra are shifted for clarity). Upper part: perpendicularly polarized incident radiation (shift: 0.1); lower part: cross-polarization (shift: 0.005).

could not experimentally be verified to the author's best knowledge, that the actual limit is indeed equal to one tenth of the wavelength nor does there exist clear evidence that there is an abrupt change of the optical properties once the crystallite size crosses the border of $\lambda/10$ up to now. To verify these heuristic assumptions, a method would be required to prepare a polycrystalline sample not only with the desired crystallite size but also with a monodisperse crystallite size distribution, conditions, which cannot be met so far. A further problem, which is also unsolved yet and connected with the preceding one, is the influence of the shape of the crystallites. As long as all dimensions are smaller or larger, respectively, than the resolution limit, it would be possibly necessary to introduce an additional weighing factor that accounts for the dependence of the fractional part a_r from the orientation of the crystallite. However, there is no approach to take into account the shape of such crystallites which possess strongly altering dimensions in different directions in space (e.g. needle shaped crystallites) with one dimension being larger than the resolution limit and with the other(s) being smaller. To make matters worse, there seems to be no experimental study of the related effects available, again possibly due to experimental limitations. As a consequence, there is no strict differentiation between the terms "diameter" and "dimension" in this work.

Overall, size distributions with $d_{max} > 5$ μm will be problematic to distinct due to the inverse proportionality between wavenumber and wavelength and the in general lower number of spectral features between the wavelengths 50–100 μm compared to the range between 10 and 50 μm.

The hypothesis of a normal distribution of crystallite sizes builds the basis of the simulated spectra depicted in Fig. 6. A consequence of this assumption is that $a_r(d)$ becomes proportional to r^3: $a_r(d) \sim r^3$, where r is the radius of the crystallite. Therefore, a dominance of the spectral features of the larger crystallites over those of the smaller ones can be inferred, which can indeed be found in Fig. 6. While the R_s spectra of the distributions with the average values of $\langle d \rangle = 1$ and 2 μm show marked differences above 300 cm^{-1}, the spectra of the distributions with the same average value $\langle d \rangle = 3$ μm but with different standard deviations $\sigma_d = 0.1$ and 0.5 μm resemble each other very closely except for small differences in the band intensities, which increase with decreasing wavenumber. Above 200 cm^{-1}, the spectra of the distributions with $\langle d \rangle = 3$ μm become gradually more similar to that of the sample consisting exclusively of large crystallites. The same is true for the cross-polarized reflectance spectra above about 370 cm^{-1}. In case of $\langle d \rangle = 1$ and 2 μm, they allow a distinction between the different values of $\langle d \rangle$ and it is also possible to discriminate between the two different values of σ_d, while the latter distinction would be difficult if $\langle d \rangle = 3$ μm, keeping in mind especially experimental limitations.

All in all, the usefulness of the method to evaluate crystallite size distributions depends on the magnitude of the optical anisotropy of the material under examination in dependence of the wavenumber.

3.3. Experimental verification

To verify the theoretical approach experimentally a polycrystalline randomly oriented sample was prepared by spark plasma sintering (SPS) with a 3:1 mass mixture of fresnoite powders consisting exclusively of small or large crystallites. Spark plasma sintering allows the preparation of high quality samples with densities close to those of the corresponding single crystals, while the crystallites can be prevented from

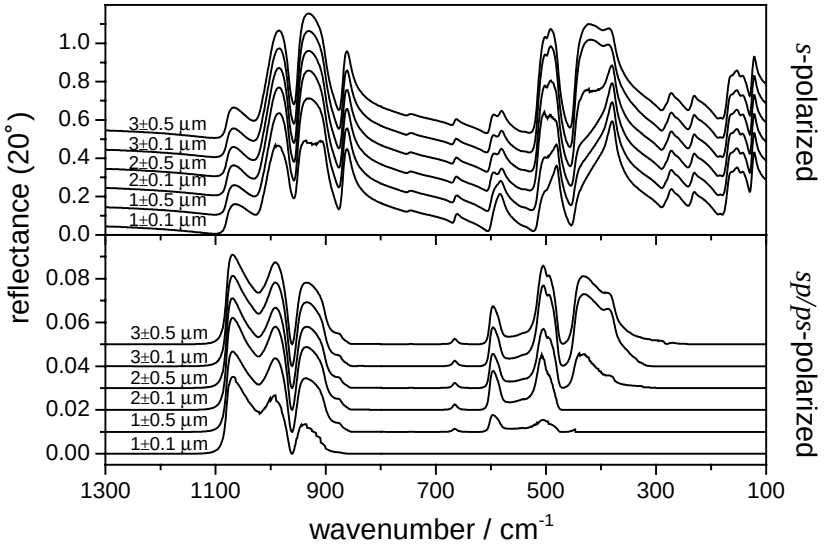

Fig. 6. Simulated reflectance spectra of randomly oriented polycrystalline fresnoite assuming normal distributions of the crystallite diameter d (incidence angle 20°, the spectra are shifted for clarity). Upper part: perpendicularly polarized incident radiation (shift: 0.01); lower part: cross-polarization (shift: 0.1).

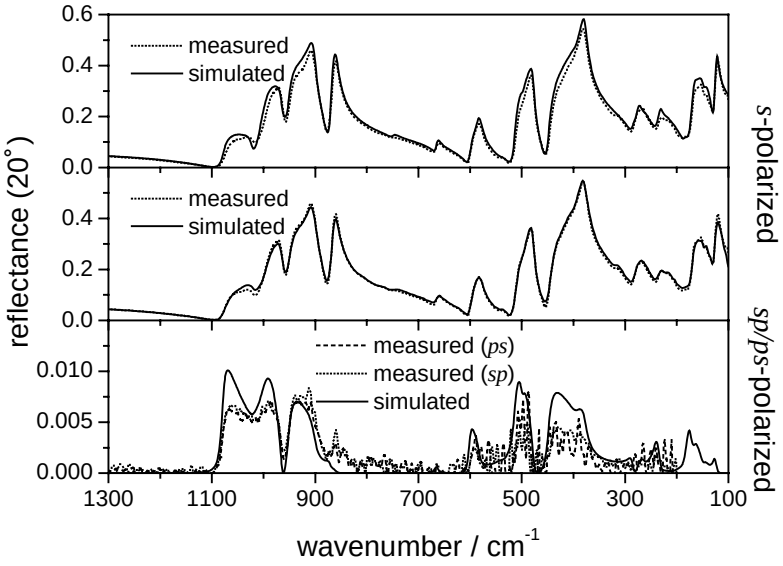

Fig. 7. Measured and simulated reflectance spectra of randomly oriented polycrystalline fresnoite prepared from a 3:1 mass mixture of powders consisting exclusively of small or large crystallites, respectively. Upper part: simulated spectrum calculated from single crystal data (perpendicularly polarized incident radiation); medium part: simulated spectrum calculated from the measured spectra of randomly oriented fresnoite consisting of small or large crystallites exclusively according to Eq. (18) (perpendicularly polarized incident radiation) and lower part: simulated spectrum calculated from single crystal data (cross-polarization spectra).

growing during the process [8]. The measured spectrum of the SPS-sample is depicted in the upper part of Fig. 7 and compared to the spectrum calculated from single crystal data according to (18) with $a_r(\text{large}) = 0.25$. Obviously, the correspondence between measured and simulated spectrum is quite satisfactorily. This correspondence is even more impressive if the measured R_s-values of the polycrystalline samples consisting exclusively of small or large crystallites are used directly in Eq. (18) instead of the simulated values (compare middle part of Fig. 7). In the lower part of Fig. 7 the comparison between the simulated cross-polarization reflectance and the measured R_{sp} and R_{ps} spectra are shown. Despite of the low intensities the comparison reveals again a satisfactory correspondence and gives further proof of the existence of a polarization conversion by an optical isotropic polycrystalline sample.

4. Summary and conclusion

A unified approach was introduced to model the spectra of randomly oriented polycrystalline bulk materials. In the main, this approach is based on two methods which have been applied for the modelling in the large (ARTT) and the small crystalline limit (ARIT). The unified approach allows the calculation of spectra of materials which possess crystallite size distributions with crystallite sizes around $\lambda/10$ and optically anisotropic crystallites. It was verified experimentally for a sample consisting of 75% per mass small and 25% per mass large crystallites. The calculated spectra for different crystallite size distributions show marked differences, which have to be taken into account if these spectra are to be interpreted. In general, however, such an interpretation is hindered by several problems. First of all, the symmetry species and therefore the principal dielectric function to which a certain vibrational band belongs cannot be evaluated without further knowledge. Secondly, the procedure to average the principal dielectric functions is time consuming even in case of the modelling. Therefore, a dispersion analysis (the extraction of the principal dielectric functions) would be much more problematic. Additional problems arise, since the crystallite size has to be taken into account. While the bands in the spectra of small crystallites show reflectance maxima near the TO-frequencies and a broadening to higher wavenumbers, the band positions in the spectra of samples consisting of large crystallites show blue shifts to higher wavenumbers in dependence of the TO–LO splitting. If a size distribution occurs a precise knowledge of the nature of this distribution would therefore be required to interpret the spectrum. All in all, the case is very comparable to the situation if optical constants shall be extracted from scattering measurements on irregularly shaped particles with anisotropic optical constants, which is yet impossible in general. As a consequence, the extraction of optical constants from bulk polycrystalline materials gives rise to serious obstacles and the evaluation of these data from a single crystal must be clearly favored.

Acknowledgements

The Author would like to thank Dr. R. Keding (Otto-Schott-Institut, FSU Jena) for the preparation of the fresnoite powders and Dr. Zhijian Shen (Department of Inorganic

Chemistry, Arrhenius Laboratory, Stockholm University) for the preparation of the SPS-sample.

References

[1] C.F. Bohren, D.R. Huffman, Absorption and Scattering of Light by Small Particles, Wiley, New York, 1983.
[2] S. Hayashi, N. Nakamori, H. Kanamori, J. Phys. Soc. Japan 46 (1976) 176.
[3] C.J. Serna, M. Ocaña, J.E. Iglesias, J. Phys. C: Solid State Phys. 20 (1987) 473.
[4] C. Pecharromán, J.E. Iglesias, Phys. Rev. B 49 (1994) 7137.
[5] M. Born, E. Wolf, Principles of Optics, Pergamon, Oxford, 1999.
[6] T.G. Mayerhöfer, Appl. Spectrosc. 56 (2002) 1194.
[7] T.G. Mayerhöfer, J. Opt. A: Pure Appl. Opt. 4 (2002) 540.
[8] T.G. Mayerhöfer, Z. Shen, R. Keding, T. Höche, Optik 114 (2003) 351.
[9] W.D.St. John, W.J. Fritz, Z.J. Lu, D.K. Yang, Phys. Rev. E 51 (1995) 1191.
[10] C. Bohley, T. Scharf, Opt. Commu. 214 (2002) 193.
[11] W. Berreman, J. Opt. Soc. Am. 62 (1972) 502.
[12] P. Yeh, Optical Waves in Layered Media, Wiley, New York, 1988.
[13] M. Schubert, Phys. Rev. B 53 (1996) 4265.
[14] I. Abdulhalim, J. Opt. A 1 (1999) 655.
[15] G.D. Landry, T. A Maldonado, J. Opt. Soc. Am. A 12 (1995) 2048.
[16] I. Abdulhalim, Opt. Commun. 157 (1998) 265.
[17] T.G. Mayerhöfer, H.H. Dunken, Vib. Spectrosc. 25 (2001) 185.
[18] T.G. Mayerhöfer, H.H. Dunken, R. Keding, C. Rüssel, Phys. Chem. Glasses 42 (2001) 353.
[19] T.G. Mayerhöfer, H.H. Dunken, R. Keding, C. Rüssel, J. Non-Cryst. Solids 333 (2004) 172.